LAWRENCE
LIVERMORE
NATIONAL
LABORATORY

LLNL-JRNL-414638

Gamma-ray multiplicity measurement of the spontaneous fission decay of 252Cf in a segmented HPGe/BGO detector array

D. L. Bleuel, L. A. Bernstein, J. T. Burke, J. Gibelin, M. D. Heffner, J. Mintz, E. B. Norman, L. Phair, N. D. Scielzo, S. A. Sheets, N. J. Snyderman, M. A. Stoyer, M. Wiedeking

July 13, 2009

Nuclear Instruments and Methods A

Disclaimer

Gamma-ray multiplicity measurement of the spontaneous fission of ^{252}Cf in a segmented HPGe/BGO detector array

D.L. Bleuel[a], L.A. Bernstein[a], J.T. Burke[a], J. Gibelin[b], M.D. Heffner[a], J. Mintz[c], E.B. Norman[a,b,c], L. Phair[b], N.D. Scielzo[a], S.A. Sheets[a], N.J. Snyderman[a], M.A. Stoyer[a], M. Wiedeking[a,b]

[a] *Lawrence Livermore National Laboratory, Livermore, California 94551*
[b] *Lawrence Berkeley National Laboratory, Berkeley, California 94720*
[c] *Nuclear Engineering Department, University of California, Berkeley, California 94720*

Abstract

Coincident γ rays from a ^{252}Cf source were measured using an array of six segmented high-purity germanium (HPGe) Clover detectors each enclosed by 16 bismuth-germanate (BGO) detectors. The detectors were arranged in a cubic pattern around a 1 μCi ^{252}Cf source to cover a large solid angle for γ-ray measurement with a reasonable reconstruction of the multiplicity. Neutron multiplicity was determined in certain cases by identifying the prompt γ rays from individual fission fragment pairs. Multiplicity distributions from previous experiments and theoretical models were convolved with the response function of the array and compared to the present results. These results suggest a γ-ray multiplicity spectrum broader than previous measurements and models, and provide no evidence of correlation with neutron multiplicity.

Keywords: fission, multiplicity, gamma-ray, neutron
PACS: 24.75.+i, 25.85.Ca

1. Introduction

The γ-ray multiplicity distribution emitted during fission is important to a number of nuclear applications. For example, significant quantitites of fissile materials may be passively detectable inside cargo by the characteristic time signature of prompt fission γ rays in several-generation chain reactions. The sensitivity of this detection technique depends on the occurrence of high multiplicity events.

There has been surprisingly little published work on γ-ray probability distributions of fissioning systems. Most studies have reported only general properties such as the average energy dissipated, the average multiplicity, or the peak multiplicity [1, 2, 3, 4]. Others have focused on more fundamental properties such as fission product angular momentum [5]. Brunson [6] attempted to determine the γ-ray multiplicity distribution of ^{252}Cf in an experiment at Los Alamos National Laboratory (LANL). However, those results suffered from a low degree

Email address: bleuel1@llnl.gov (D.L. Bleuel)

of detector segmentation. Multiplicities as large as 20 were inferred by fitting a double Poisson distribution to data taken with only eight detectors. Recent Monte Carlo simulations [7], also conducted at LANL, have predicted good, but not exact agreement with this experiment as shown in Fig. 1. The discrepancies are especially significant at high multiplicities.

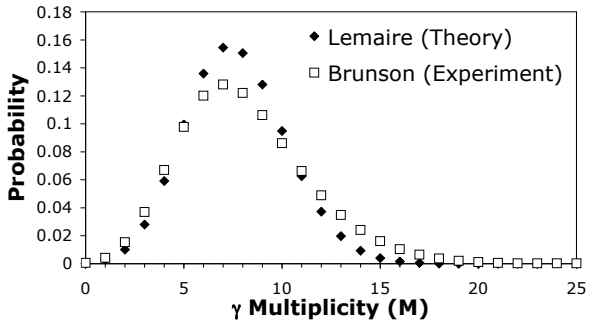

Figure 1: Brunson [6] and Lemaire *et al.* [7] γ-ray multiplicity distribution for ^{252}Cf spontaneous fission.

Furthermore, little is currently known about the relationship between γ-ray multiplicity and neutron multiplicity in the fission process. In fact, competing theories predict opposite correlations between the two. The LANL theory [7] predicts that γ-ray multiplicity decreases with increasing neutron multiplicity. A new, LBNL-developed, preliminary Monte Carlo code, FREYA [8], (Fission Reaction Event Yield Algorithm), predicts anti-correlation between neutron multiplicity and fission product excitation energy. Given that the average γ-ray energy is roughly independent of neutron multiplicity [9], this suggests that higher excitation energy produces higher γ-ray multiplicity. Conversely, earlier experiments [1, 9, 10] have revealed a positive correlation between γ-ray and neutron multiplicities, as both arise from initially highly-excitated systems with low recoil velocity. No attempt has yet been reported to measure this correlation for specific pairs of fission fragments.

Confirming the validity of the LANL theoretical model with an easily-tested ^{252}Cf spontaneous-fission source gives confidence in using the model to predict more relevant neutron-induced multiplicity distributions for uranium and plutonium.

Many studies of the prompt and delayed γ rays emitted following spontaneous fission of ^{252}Cf and ^{248}Cm utilizing large arrays of germanium detectors have been performed over the past two decades. A review of many of the experiments from the early 1960s through the mid 1990s can be found in Hamilton *et al* [11]. Spontaneous fission studies in Gammasphere, an array of 110 high-purity germanium (HPGe) detectors, included ^{252}Cf [12] and ^{242}Pu [13]. Eurogam, an array of more than 50 HPGe detectors located at various laboratories in Europe, concentrated on ^{248}Cm [14]. Almost all of these experiments were performed in anticipation of studying the nuclear structure of prompt neutron-rich fission

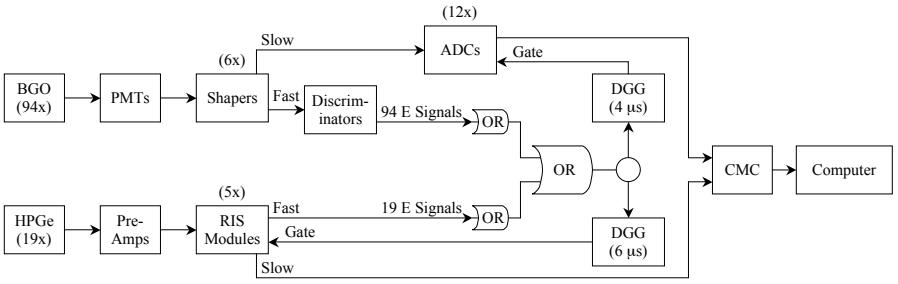

Figure 2: Schematic of the signal processing electronics (see text).

fragments. It should be noted that the fission of ^{252}Cf, ^{248}Cm and in particular, ^{242}Pu, have different distributions of fission fragments, enabling the detailed study in some cases of different nuclides. Indeed, many results on nuclei that cannot be studied by any other technique than fission have been published and continue to be published today from these rich data sets [15, 16, 17, 18, 19, 20]. A few studies also investigated the dynamics of fission [21, 22, 23] or ternary fission [24]. None of these experiments was optimized to easily study the multiplicity and total energy of γ rays emitted per each fission event.

An attempt was made in 2006-2007 to "mine" the copious amounts of spontaneous fission data from Gammasphere and obtain γ-ray multiplicity distributions on an event-by-event basis [25]. Prior Gammasphere experiments had been configured to trigger on three or more clean HPGe events. In addition, these experiments were not configured to collect calorimetric information and hevimet shields were installed on the BGO Compton suppression detectors, reducing the efficiency of collecting γ-ray multiplicity information from nearly 100% to approximately 10%. Finally, "dirty" BGO events or BGO-only events were not recorded for future analysis at all. Thus, large corrections would be required to obtain multiplicity distributions from these data sets. This clearly indicated a need for an experiment optimized to obtain $\gamma-$ray multiplicity distributions.

2. Experiment

2.1. Apparatus

The experiment was performed using six EURISYS high-purity germanium (HPGe) "Clover" [26] detectors of the Livermore-Berkeley Array for Collaborative Experiments (LiBerACE) at the 88-Inch Cyclotron at Lawrence Berkeley National Laboratory (LBNL). Each Clover consists of four HPGe crystals in a shared cryostat surrounded by 16 SCIONIX bismuth-germanate (BGO) [27] detectors. These six HPGe/BGO detector modules were mounted along orthogonal axes with their front faces edge-to-edge in a cubic pattern as in Fig. 3. This geometry provided good solid angle coverage, a high degree of segmentation (potentially 24 HPGe and 96 BGO detectors, though 5 HPGe and 2 BGO

elements were not operational during data collection) and the ability to identify specific isotopes due to the high resolution of HPGe.

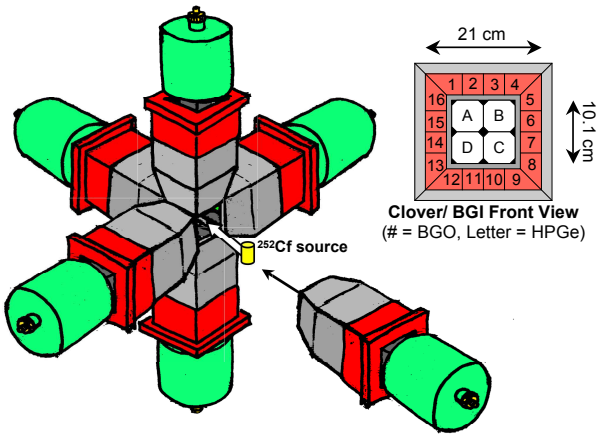

Figure 3: (Color online) Schematic representation (not to scale) of detector arrangement, with ^{252}Cf source about to be placed at the center.

Leaded, borated polyethylene bricks surrounded the four table-mounted horizontal-plane detectors to reduce room background.

Figure 2 shows schematically how the individual HPGe and BGO signals were processed by the data acquisition system. Scintillation light from the BGO crystals was detected using 94 individual Hamamatsu R6094 photomultiplier tubes (PMTs) and amplified by six 16-channel CAEN N568B shaping amplifiers. The gains were matched by adjusting the PMT bias voltages between ∼1100–1400 V. The 94 "fast" timing signals of the shaping amplifiers were connected to LeCroy 1806 leading-edge discriminators. The 19 HPGe signals were processed by five RIS Model 1200 modules [28], also in use at Oak Ridge National Laboratory's CLARION array [29], which consist of shaping amplifiers, constant fraction discriminators (CFDs) and analog-to-digital converters (ADCs). The "fast" output signals from these modules were combined with those from the BGO discriminators in LeCroy 429A logic modules requiring only one or more signals to trigger an event ("OR" mode). This trigger was split and used to generate gates for the ADCs using two delay-gate generators (DGGs). When a valid trigger occurred, the first gate generator produced a 6 μs gate for the digitization of the HPGe signals by the RIS module. The second gate generator produced a 4 μs gate for twelve 8-channel SILENA 4418/U ADCs, into which the "slow" BGO output signals from the CAEN shapers were fed. Finally, the digitized FERA signals were mixed together with CMC204 modules, buffered using a CMC203 histogramming memory module, and read out by a customized KMAX data acquisition system. A 100-keV software threshold was set on both the BGO and HPGe energies during analysis.

Table 1: Array detection efficiencies calculated from calibration sources, including the total array efficiency, ϵ_{tot}, and partial efficiencies of each component of the array, ϵ_{BGO} or ϵ_{HPGe}. M is the source multiplicity, E_γ is the γ-ray energy, A is the source activity, and BR_γ is the gamma-emission branching ratio. For the two-gamma ^{60}Co source, the energy-averaged single-photon efficiency, $\overline{\epsilon_1}$, is directly comparable to ϵ_{tot} of the single-photon sources (see text). Measured detection rates were divided by the acquisition system live time fraction and background-subtracted. Statistical uncertainties were insignificant. Because some events trigger both HPGe and BGO detectors, $\epsilon_{tot} < \epsilon_{BGO} + \epsilon_{HPGe}$.

Source	M	E_γ	$A \cdot BR_\gamma$	Measured Rate	ϵ_{tot}	ϵ_{BGO}	ϵ_{HPGe}	$\overline{\epsilon_1}$
^{137}Cs	1	662 keV	0.712 μCi	1.39×10^4 Hz	53%	43%	15.7%	
^{54}Mn	1	835 keV	0.0115 μCi	2.29×10^2 Hz	54%	42%	15.4%	
^{60}Co	2	1173 keV 1333 keV	0.483 μCi	1.41×10^4 Hz	79%	73%	28.6%	54%

2.2. Data Acquisition

A 1-μCi ^{252}Cf liquid (1 ml) source was placed at the center of this array. Data was recorded for one week. This source, with a 3.1% spontaneous-fission branch, underwent 1150 fissions per second, i.e. about 7×10^8 fission events in one week. Room background was measured for two days. The array response was measured using six calibration sources (^{152}Eu, ^{60}Co, ^{137}Cs, ^{228}Th, ^{54}Mn, ^{22}Na) in the range of 0.01-1.0 μCi.

The acquisition system was set to trigger on single photons and record all coincident photons detected within a 2 μs (BGO) or 2.7 μs (HPGe) time window from the triggering event (set to peak near the center of the 4 or 6 μs gates). With the ^{252}Cf source at the center of the array, the total count rate was approximately 6500 Hz. This includes γ rays from spontaneous fission, beta decay of fission products (known as "beta-delayed gammas"), and room background sources (2760 Hz). At this rate, within a 2 μs timing window, 1.3% of detected events are uncorrelated ("randoms") with the triggering γ ray. Within the 2.7 μs HPGe timing window, the random rate is 1.8%.

Table 1 shows the total efficiency of the array (ϵ_{tot}) for detecting at least one photon (not necessarily the full photopeak) from some of the calibration sources with simple decay schemes. The array naturally has a higher efficiency for detecting one photon from a multiple-photon source such as ^{60}Co than for a single-photon source. Assuming isotropic emission and energy-independent efficiency, an effective single-photon detection efficiency can be calculated from the total efficiency, ϵ_{tot}, for ^{60}Co.

The efficiency, ϵ_M, for detecting at least one γ ray from a source emitting M uncorrelated, monoenergetic photons obeys the simple probability relation:

$$\epsilon_M = 1 - (1 - \epsilon_1)^M \tag{1}$$

where ϵ_1 is the efficiency for detecting a single-photon source of a given energy. Solving for ϵ_1,

$$\epsilon_1 = 1 - (1 - \epsilon_M)^{\frac{1}{M}} \quad (2)$$

we can determine the effective single-photon efficiency for the ^{60}Co source, which emits exactly two γ rays (1173 keV and 1333 keV) in 99.9% of beta decays. [30] The value in Table 1 is $\overline{\epsilon_1}$, the energy-averaged single-photon efficiency using ϵ_{tot} for ϵ_M.

The detection efficiency of the array for a single 662-keV γ ray is 53% and does not appear to change significantly with increasing energy up to at least 1332 keV. The ratio of the BGO detection efficiency to that of the HPGe is also nearly constant over these energies at 2.8 to 1.

As a test of the triggering efficiency, $\overline{\epsilon_1}$ can be directly compared to the efficiency of the array for detecting one ^{60}Co γ ray in coincidence with the other. When gating on the 1173-keV γ-ray photopeak in an HPGe detector, the efficiency of the remainder of the array to detect at least one additional γ ray is 66% (or 67% when gating on the 1333-keV γ-ray photopeak). This is significantly higher than the energy-averaged single-photon efficiency ($\overline{\epsilon_1}$) of 54% calculated from Eq. 2. Unfortunately, this is the result of some of the BGO leading edge discriminators which determined the trigger condition having been set higher than the corresponding ADC lower level discriminators and the 100-keV software threshold set during analysis. In other words, a photon depositing low energy in a given BGO might not trigger the array alone, but would be counted if another element triggered the array. While this can have a dramatic effect when comparing "raw" multiplicity spectra with "gated" spectra (in coincidence with a given energy γ ray in an HPGe element), the effect is minimized at high multiplicity ($M > 5$) where the array triggering efficiency approaches one. For separate reasons, discussed later, our analysis has been restricted to high-multiplicity events where this effect is negligible.

Table 2: Percentage of photon energy gates (E_G) in coincidence solely with response function photon energies (E_R) and with all other contaminant decay chains, grouped by multiplicity (M). Values are determined from known beta, γ ray, and internal conversion transitions in the ENSDF [30] database. Values in the "$M = 1$" column represent coincidences of E_G with a single γ ray, but not of energy E_R.

Source	E_G (keV)	E_R (keV)	Coincident Fraction	Contaminant decays			
				$M = 0$	$M = 1$	$M = 2$	$M = 3$
^{152}Eu	779	344	95.8%	3.8%	0.02%	0.4%	
^{60}Co	1333	1173	99.9%	0.1%	<0.01%	<0.01%	
^{60}Co	1173	1333	100.0%	<0.01%			
^{228}Th	861	2614	97.4%	0.2%	0.7%	1.6%	0.02%

3. Data analysis

Two factors primarily affect the difference between the actual source multiplicity, M, and the detected source multiplicity, M': detector array efficiency

and γ-ray multiplication from pair production and Compton scattering. Lower detector array efficiency lowers M' relative to M. Pair production and Compton scattering processes, in which energy from a single photon is deposited in two or more detectors, raise M'. Rather than unfold our detected M' distribution to determine a source M distribution, we compared our results with experimental and theoretical M distributions by convolving them with the response function of our array.

To determine this response function at various source photon energies, we used calibrated sources with two-photon-only decay branches, such as ^{60}Co, which emits exactly two photons of 1173 keV and 1333 keV 99.9% of the time following beta decay. When the full energy of one of these photons is detected in a HPGe detector, we know that the other γ ray was simultaneously emitted into 4π. Thus, the response of the remainder of the array to a single photon of the other energy is determined. Grouping M such single-photon-response events together simulates an M-multiplicity source of monoenergetic photons, consisting of a cascade of M γ rays. The events were grouped together such that photons from different events in the same detector add only one to the total detected multiplicity. In this procedure, we neglect the effect of γ–γ angular correlations in calibration sources.

The response function to four energies (344 keV, 1173 keV, 1333 keV, and 2615 keV) was determined using three calibration sources (^{152}Eu, ^{60}Co, and ^{228}Th). Of the decays in coincidence with the gated energy, E_G, the fraction which emit only a single additional photon of the response function energy, E_R, is listed in Table 2. Internal conversion and higher-level feeding in beta decay can lead to the emission of E_G not solely in coincidence with E_R. Table 2 also lists the percentages of these contaminant decays that are in coincidence with E_G.

To subtract the contribution from background events (primarily from Compton scattering of higher energy photons), a single-photon response function was generated from data selected just adjacent to the gated photopeak energy. Then, when grouping together M single-photon events to create an M-photon response function, some events that would normally contribute N detected γ rays were omitted. The fraction of these events omitted was the ratio of counts in the off-peak single-photon response function to the on-peak response function for events of detected multiplicity N.

While the random rate for the array was small, event-grouping compounds the contribution from random events, increasing its significance in higher multiplicity response functions. A similar routine as that used to subtract Compton background events was used to subtract random coincidences (from the source or room background) during the acquisition time gates. The random fractions from multiple source decays were determined from the known source strengths and gate times. The random fraction from room background was determined from the number of decays observed in coincidence with 1461-keV γ rays from ambient ^{40}K (a single-photon room background decay).

The four response functions are plotted for two values of M ($M = 1$ and 10) in Fig. 4. The response function appears to differ only slightly as a function of

photon energy, most notably at the lowest energy of 344 keV. This difference lessens as the source multiplicity increases.

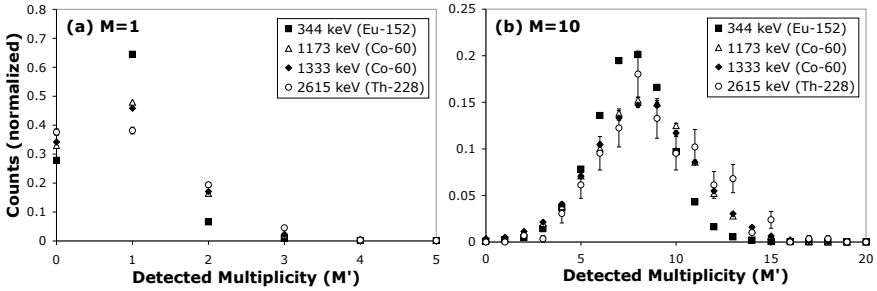

Figure 4: The detected multiplicity (M') response function for a source multiplicity of (a) $M = 1$ and (b) $M = 10$. The functions are normalized to sum to unity over all multiplicities. Where not indicated, statistical error bars are smaller than the data points.

Figure 5 shows the γ-ray spectrum of ^{252}Cf seen by the HPGe detectors, divided into four regions above a 100-keV threshold. The borders of these regions correspond to the midpoints between the four energies at which the response functions were calculated.

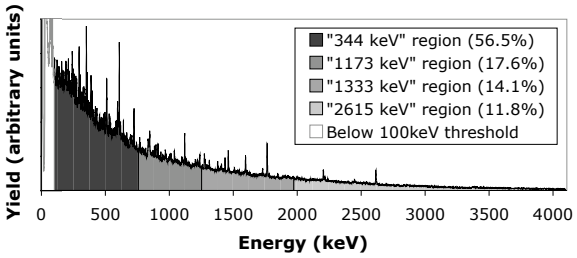

Figure 5: Energy efficiency-corrected HPGe spectrum. The borders of each region are the midpoints between the four response function energies, with the percentage of yield in each region indicated in the legend.

Since a ^{252}Cf fission source is not monoenergetic, it may be inappropriate to characterize the ^{252}Cf response solely by any of the single-energy response functions from Fig. 4. An energy-dependent response function for the ^{252}Cf fission source was estimated by summing the four single-energy response functions for each source multiplicity, weighted by the fraction of the spectrum detected in these four regions. It should be noted that this method overestimates the contribution of lower energies, as the detected source spectrum includes some incomplete photon energy deposition from Compton scatter. This response reflects a lower bound, while a monoenergetic response at one of the higher energies produces an upper bound.

4. Overall gamma multiplicity

The detected multiplicity spectrum (M') in Fig. 6 shows four main sources of γ rays: room background, cosmic-ray background, fission-product beta decays, and fission events.

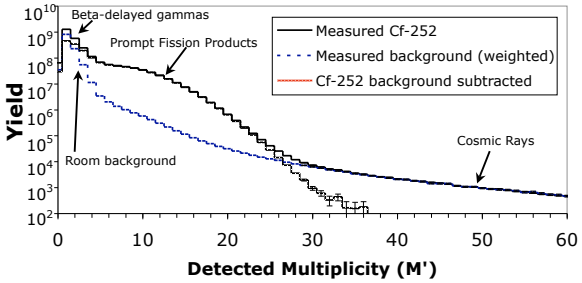

Figure 6: (Color online) Measured multiplicity spectra on a logarithmic scale to show all features. Error bars, representing only statistical uncertainty, were omitted when smaller than the data line. The background data was weighted by the ratio of ^{252}Cf to background data acquisition times.

Room and cosmic-ray backgrounds are easily subtracted by counting with no source present. The agreement of these spectra in the very high multiplicity region ($M' \gtrsim 30$), dominated by cosmic-ray interactions, gives high confidence to this background subtraction.

Most of the photons detected were from beta decay of the fission products. These are overwhelmingly low-multiplicity events ($M \lesssim 3-4$). There is no way to distinguish these events from fission events. However, we are reasonably confident that the probability of detecting $M' > 7$ from a fission product beta decay is negligible, and we restrict our comparisons to this region. This assumption was tested using two different methods. The first method was the observation of a specific beta decay while the second method attempted to characterize the entire beta-delayed multiplicity spectrum from known decay data and gamma cascades in the ENSDF library [30].

In the first method, we observed the multiplicity of the array during the beta decay of ^{108}Rh or ^{108m}Rh to ^{108}Pd, a stable fission product with a very low direct fission population. The direct population of ^{108}Pd in ^{252}Cf spontaneous fission is only 0.00061% [31]. The cumulative population from both direct population and beta decay chains of other fission fragments is 6.1%, a factor 10^4 larger. The decay was determined by the observation of the 434-keV $2^+ \rightarrow 0^+$ γ-ray transition in ^{108}Pd in one of the HPGe crystals. Background was determined by gating on a nearby energy region clean of discrete γ-ray peaks from other isotopes and subtracted. Similarly, the spectrum from ^{106}Mo, a primarily directly-populated fission fragment, was obtained by gating on its 172-keV $2^+ \rightarrow 0^+$ transition. ^{106}Mo is directly populated in 3.5% of ^{252}Cf spontaneous fissions, 90% of its cumulative population of 3.9% [31]. The multiplicity spectra

for each of these products is shown in Fig. 7. The spectra are slightly biased to lower multiplicities by gating on a specific energy γ ray in an HPGe detector since they do not include Compton scatters of that γ ray. However, correcting this bias would not increase the high-multiplicity region significantly, as it drops quickly to nearly zero at multiplicities greater than 6. The ^{106}Mo off-peak background subtraction actually contained a small contribution from a beta-delayed product of ^{139}Cs which is the reason the spectrum falls below zero at low multiplicity. The higher multiplicity yields appear unaffected, demonstrating further evidence that beta-delayed γ rays do not contribute significantly to high multiplicities. However, this tested only a single representative beta-delayed fission product.

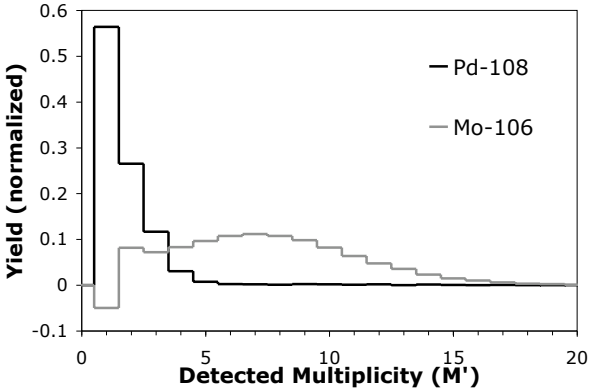

Figure 7: Measured multiplicity spectra gated on a γ ray from ^{108}Pd (434 keV) and from ^{106}Mo (172 keV). The yields are normalized to sum to unity over all multiplicities.

In the second method, full decay chains for every known beta-delayed fission product were created from the ENSDF library. Multiplicity spectra for each isotope were generated and added together, weighted by their beta-delayed yields. Nuclear levels with half-lives greater than our BGO gate time of 4 μs were neglected. Thirty isotopes with beta-decay half-lives longer than one year were not included. Conversion electrons and γ rays below a 100-keV threshold did not contribute to a decay chain's multiplicity. For the 253 isotopes with beta decay yields over 0.1%, 165 decay chains were generated successfully, 70 had no ENSDF beta decay data, and 3 failed to identify energy levels in over 5% of that isotope's yield. The resulting multiplicity spectrum from the 362 total successful decay chains (including all yields) is shown in Fig. 8(a). This spectrum convolved with both a low-energy (344 keV) and a high-energy (1333 keV) detector response function is shown in Fig. 8(b). Again, there is negligible yield at multiplicities higher than 6.

To reproduce the detected multiplicity spectra (M') that the LANL experiment [6] and theory [7] would produce in our array, the multiplicity spectra (M) from Fig. 1 were folded with the spectrum-weighted response functions described above. These convolved spectra are compared to with our measured

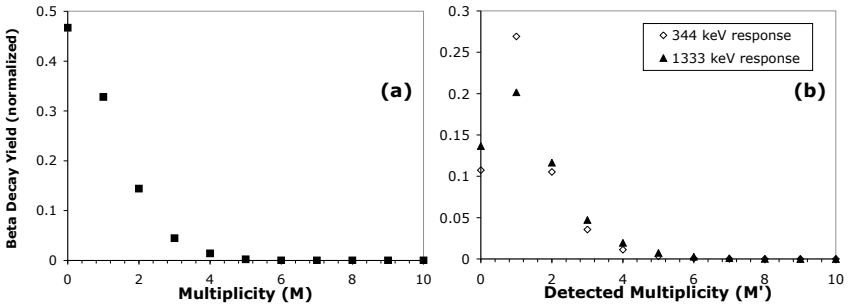

Figure 8: (a) Multiplicity spectrum determined by following all possible known beta-gamma decay chains in ENSDF and (b) this spectrum convolved with the array response function at 344 keV and at 1333 keV. $M' = 0$ represents only detected events below the 100-keV software threshold. Error bars are omitted as ENSDF does not report uncertainties. The yields are normalized to sum to unity over all multiplicities.

M' spectrum in Fig. 9. Because the HPGe energy spectrum from Fig. 5 is low-energy weighted compared to the actual fission spectrum, we also compared our measured results with the LANL experiment and theory folded with the array response function at 1333 keV. This is nearly identical to the responses at both 1173 keV and 2615 keV and overestimates the multiplicity spectrum as an upper bound.

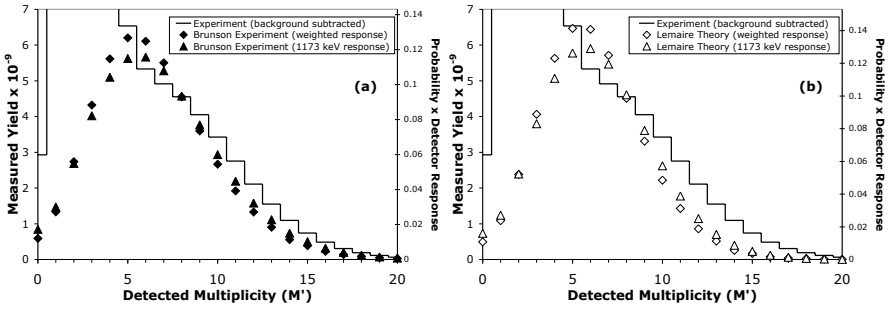

Figure 9: Comparison of our measured multiplicity spectrum (line, left x-axis) with (a) the LANL experiment [6] and (b) the LANL theory [7] as they would be seen in our detector array (datapoints, right x-axis) using two different response functions. Axes have been scaled to match at $M' = 8$, where the contribution from beta-delayed gammas is expected to be negligible.

While the beta-delayed gamma spectrum makes it difficult to quantify, it appears the centroid of our measured spectrum is similar to those being compared. However, in the $M' > 7$ region, both the LANL experiment and theory drop off more rapidly with higher multiplicity than our measurement, reaching zero yield at $M' = 20$. This difference appears slight when comparing to a higher-energy response function of the LANL experiment, though the centroid

at $M' = 7$ should be lower than measured in this work due to beta-delayed γ ray contamination.

This suggests that the actual multiplicity spectrum (M) from ^{252}Cf fission may be somewhat broader than previously measured and significantly broader than that predicted by theory. However, we are restricted to comparisons in the "uncontaminated" region of high multiplicity. A similar experiment with a fission detector, or an alternate method of differentiating beta-delayed gammas from prompt fission γ rays, would eliminate the low M background and yield more quantitative results. Future experiments should employ such techniques.

5. Gamma Multiplicity as a Function of Neutron Multiplicity

The high resolution of the HPGe detectors allows identification of specific fission products by the observation of emitted γ ray energies from known transitions in those nuclei. A simple subtraction of the neutron numbers in two uniquely identified fission fragments from the original number of neutrons in ^{252}Cf gives the neutron multiplicity of each event.

Such measurements face a number of challenges. Figure 5 shows that there is a very high background, primarily from Compton scatters of higher energy fission γ rays and a continuous spectrum of statistical decays of highly-excited nuclei. Because of the very large number of possible fission fragments, there is also a very high discrete γ-ray density, with many overlapping peaks. This issue is compounded because isotopes that differ only by a neutron pair often have similar transition energies.

We restricted our fission fragment search to deformed nuclei with both even numbers of protons and neutrons ("even-even" nuclei) with strong ground-state rotational γ-ray band transitions. Some potential candidates from ^{252}Cf fission include Mo/Ba, Ru/Xe and Zr/Ce pairs. Of these isotopes, only the Mo/Ba pairs were populated strongly enough to obtain sufficient statistics to attempt discerning any differences in γ-ray multiplicity. Unfortunately, both the $2^+ \rightarrow 0^+$ and the $4^+ \rightarrow 2^+$ transitions of ^{104}Mo (192 keV, 369 keV) and ^{108}Mo (193 keV, 371 keV) are too close in energy to be sufficiently differentiated. Higher-spin states are not as frequently populated and decay by higher γ-ray energies with lower efficiency for full photopeak energy deposition in HPGe detectors. The most common even-even ^{106}Mo/^{x}Ba fragment pairs [11] are listed in Table 3, along with the energies of their lowest-spin rotational band transitions. Only the ^{106}Mo/^{144}Ba and ^{106}Mo/^{142}Ba pairs were of sufficient yield, representing, respectively, the emission of 2 and 4 neutrons. The 199.3 keV $2^+ \rightarrow 0^+$ γ ray from ^{144}Ba overlaps several γ rays emitted from ^{143}Ba. Therefore, only the $4^+ \rightarrow 2^+$ transitions in barium isotopes were used. The 332-keV $4^+ \rightarrow 2^+$ γ ray from ^{146}Ba is similar to the 331-keV $4^+ \rightarrow 2^+$ γ ray from ^{144}Ba. This energy difference is greater than the HPGe detector resolution and the small portion of the tail of the much weaker ^{146}Ba peak that overlaps the ^{144}Ba gate only increases the difference in the average number of emitted neutrons versus ^{142}Ba.

Table 3: Neutron multiplicities (ν), yields (per 100 ^{252}Cf spontaneous fissions), and ground-state rotational band γ-ray energies in keV (E_γ) of the most common correlated even-even ^{106}Mo/^{x}Ba fission fragment pairs (FF1 and FF2 from column 1), from Hamilton *et al.* [11].

	Fragments		FF1 E_γ		FF2 E_γ	
ν	(FF1/FF2)	Yield	$(2^+ \rightarrow 0^+)$	$(4^+ \rightarrow 2^+)$	$(2^+ \rightarrow 0^+)$	$(4^+ \rightarrow 2^+)$
0	^{106}Mo / ^{146}Ba	0.08(5)	172	351	181	332
2	^{106}Mo / ^{144}Ba	0.65(4)	172	351	199	331
4	^{106}Mo / ^{142}Ba	0.92(4)	172	351	360	475
6	^{106}Mo / ^{140}Ba	0.12(3)	172	351	602	528

The LANL theory predicts the γ-ray multiplicity distributions (M) for 2-neutron and 4-neutron emission fission as shown in Fig. 10(a). Figure 10(b) shows the multiplicity distribution that our detector array would see from each source (M') after being convolved through the fission spectrum-weighted response function. The widths of each distribution are similar, but the centroids differ by two. If the LANL theory is correct, we expect to be able to discern the difference between a 2-neutron and a 4-neutron fission by this shift in centroid. An almost identical shift is seen if these spectra are folded with any higher-energy (1173 keV, 1333 keV, or 2615 keV) detector response function.

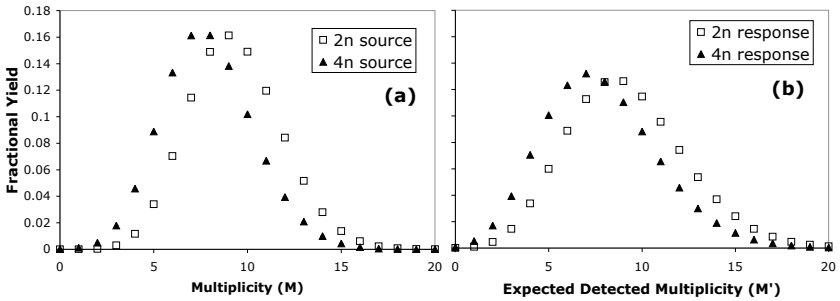

Figure 10: (a) Fission γ-ray multiplicity spectra (M) for two neutron multiplicities as predicted by the LANL theory [7], and (b) multiplicity spectra that would be detected by our array (M'), generated by convolving M with the fission spectrum-weighted detector response function.

As previously noted, most of the γ rays detected at a given energy are not from the discrete fission fragment transition in which we are interested, but from "background" such as Compton scattering of higher-energy γ rays and continuous-spectrum "statistical" decays. Typically, an equivalent-width energy gate near the peak of interest will yield the same background sources and can be subtracted from the on-peak energy gate. Double-gating on two peaks of interest incurs a somewhat more complex background subtraction technique.

A portion of the γ-ray energy spectrum detected by the HPGe detectors is shown in Fig. 11. ^{106}Mo and ^{142,144}Ba peaks are labeled by their energies. Many beta-delayed γ-ray peaks are significantly reduced when two or more hits

are required in the HPGe detectors. The barium γ rays in coincidence with the 172-keV ^{106}Mo peak are predictably more prevalent but are still weaker than background sources. The prevalence of the remaining 172-keV ^{106}Mo peak in coincidence with other 172-keV γ rays is indicative of this large background fraction. A significant fraction of the Compton-scattered background events is eliminated by not including γ rays coincident with each gate in crystals from the same Clover detector. A similar effect could be accomplished by adding together energies in adjacent Clover elements. However, incomplete energy deposition is small at the energies of interest (less than ~500 keV) and this introduces a larger suppressive bias of high-multiplicity events due to "pile-up," when multiple γ rays hit the same detector.

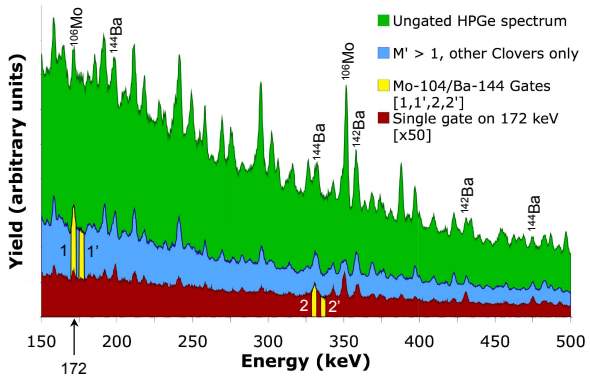

Figure 11: (Color online) A portion of the ^{252}Cf γ-ray spectrum detected in HPGe detectors, showing the full spectrum, the spectrum in coincidence with at least one other HPGe-detected γ ray, and the spectrum in coincidence with a 172-keV γ ray (multiplied by 50), designated gate "1." The latter two spectra do not include γ rays from the same Clover detector. On-peak and off-peak portions of each spectrum for which double-gated coincidence multiplicity spectra are generated in the example in the text are labeled 1, 1′, 2, and 2′.

An example of on-peak gates of the ^{106}Mo/^{144}Ba pair is shown in Fig. 11 and are numbered 1 and 2, with off-peak gates labeled 1′ and 2′. Gating on two of these coincident energies selects events which include both "peaks" (the full photopeak of γ rays from discrete transitions) and "backgrounds" (locally energy-independent non-discrete sources from Compton scattering or "statistical" decays from isotopes selected by the other gate). It is assumed that background from a particular isotope is the same at a given gate and its off-peak gate. For instance, the portion of Gate 1 that is a 172-keV γ ray from ^{106}Mo contributes equal background at Gates 2 and 2′. It is also assumed that a given isotope with a peak at a given gate does not have a peak at any of the other gates.

The double-gated multiplicity spectrum from fission events producing only ^{104}Mo and ^{144}Ba coincident prompt fission fragments (M'_A) is then

$$
\begin{aligned}
M'_A &= M'_{1,2} - M'_{1,2'} - (M'_{1',2} - M'_{1',2'}) \\
&= M'_{1,2} - M'_{1,2'} - M'_{1',2} + M'_{1',2'} \qquad (3)
\end{aligned}
$$

where $M'_{x,y}$ is the multiplicity spectrum generated when gating on both energy regions x and y in two different HPGe detectors, either on-peak (1 or 2) or off-peak ($1'$ or $2'$) as illustrated in Fig. 11. Equation 3 is applicable to any fission product pair with gates at appropriate x and y energy regions. The background-corrected multiplicity spectra generated from this method for the ^{106}Mo/^{142}Ba and ^{106}Mo/^{144}Ba pairs are shown in Fig. 12.

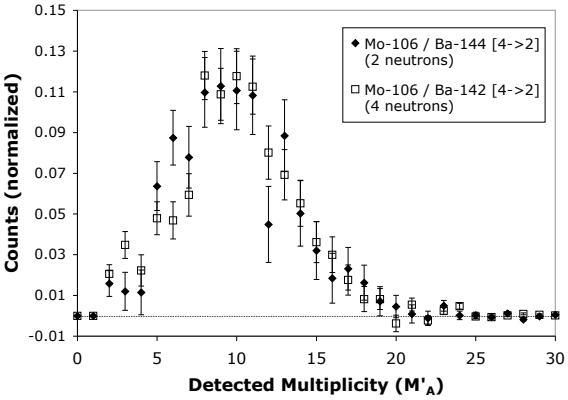

Figure 12: Normalized γ-ray multiplicity spectra (M'_A) detected for a two-neutron (diamonds) and a four-neutron (squares) emission fission into Mo and Ba. Error bars represent statistical uncertainty only. The functions are normalized to sum to unity over all multiplicities.

The multiplicity spectra, M'_A, in Fig. 12 do not accurately represent the true source multiplicity spectra, M, or even the detected multiplicity spectra, M'. Generating these spectra introduces several multiplicity-dependent biases. For instance, the efficiency for detecting a higher-multiplicity event is decreased due to "pile-up" when more than one γ ray hits a given HPGe detector. Furthermore, requiring at least two detected γ-rays biases higher-multiplicity events (with a zero probability of detecting $M'_A = 1$). However, this bias is negated if Eq. 3 appropriately removes all contributions except for the two γ rays of interest, and the probability of a given fission fragment emitting one of these low-lying rotational band transitions is not multiplicity dependent. To further minimize bias from any multiplicity-dependent rotational band level feeding, we have chosen to compare only the same J^π transitions ($4^+ \rightarrow 2^+$) for each barium isotope.

While the multiplicity spectra shown in Fig. 12 are not perfectly comparable to those of Fig. 10 due to these biases, the predicted centroid shift nevertheless should be readily apparent. However, no apparent difference in γ-ray multiplicity spectra is observed, especially in the higher-multiplicity region where the

bias from forcing a double HPGe gate is expected to have a minimal effect. The mean detected multiplicities ($\overline{M'_A}$) for the two-neutron and four-neutron emission fission events in Fig. 12 are equal, respectively 9.9(0.7) and 9.9(0.5). The normalized chi-squared difference (χ^2/ν) between the two distributions is 1.00, indicating perfect agreement within the uncertainties. However, χ^2/ν of only the low-multiplicity (M'_A=2–8) portion of the distributions is higher (2.2) reflecting disagreement in this region, while χ^2/ν of the high-multiplciity (M'_A=8–25) is lower (0.49) indicating agreement better than expected from the uncertainties in this region. It should be noted that the statistical uncertainty stemming from the considerable background subtractions is large. These observations should therefore be considered cautiously.

The apparent independence of γ-ray multiplicity from neutron multiplicity suggested by these results is surprising, supporting neither correlation [1, 9, 10] nor anti-correlation [7, 8] theories or observations. However, we observed only the difference between two specific pairs of fission fragments whereas those previous studies predicted or observed average trends across all fissioning systems. Therefore, further study examining a greater variety of fission fragment pairs is desirable to fully support either trend as well as any fragment dependence.

6. Summary

We have measured the γ-ray multiplicity of ^{252}Cf spontaneous fission in a highly-segmented detector array consisting of BGO and HPGe detectors. The overall multiplicity measured is in good agreement with a previous low-segmentation experiment, but suggests a slightly broader high-multiplicity tail. We selected pairs of fission products from their characteristic γ rays in high-resolution HPGe detectors to determine the γ-ray multiplicity dependence on neutron multiplicity. Despite the uncertainty due to high background effects and potential biases introduced in the event selection, there was no discernible difference in the γ-ray multiplicity between the 2-neutron (^{106}Mo/^{144}Ba) and 4-neutron (^{106}Mo/^{142}Ba) emission fission events.

7. Acknowledgments

This work was performed under the auspices of the U.S. Department of Energy by Lawrence Livermore National Laboratory in part under Contract W-7405-Eng-48 and in part under Contract DE-AC52-07NA27344 and the U.S. Department of Energy by Lawrence Berkeley National Laboratory under Contract No. DE-AC02-05CH11231.

References

[1] P. Glässel, R. Schmid-Fabian, and D. Schwalm, Nucl. Phys. A502 (1989) 315c.

[2] E. A. Sokol, G. M. Ter-Akop'yan, A. I. Krupman, V. P. Katkov, L. F. Nikonova, and N. V. Eremin, Sov. J. At. Energy 71 (1991) 906.

[3] V. S. Ramamurthy, R. K. Choudhury, and J. C. Mohan, Pramana 8 (1977) 322.

[4] R. Varma, G. K. Mehta, R. K. Choudhury, S. S. Kapoor, B. K. Nayak, and V. S. Ramamurthy, Phys. Rev. C 43 (1991) 1850.

[5] J. B. Wilhelmy, E. Cheifetz, R. C. Jared, S. G. Thompson, H. R. Bowman, and J. O. Rasmussen, Phys. Rev. C 5, (1972) 2041.

[6] G. S. Brunson, Ph. D. Thesis, University of Utah, Los Alamos National Laboratory Report No. LA-9408-T, 1982.

[7] S. Lemaire, P. Talou, T. Kawano, M. B. Chadwick, and D. G. Madland, Phys. Rev. C 72 (2005) 014602.

[8] R. Vogt and J. Randup, in *Proceedings of the Workshop on Compound-Nuclear Reactions and Related Topics, Yosemite National Park, CA, 2007*, edited by J. Escher (Lawrence Livermore National Laboratory, 2008), 202.

[9] H. Nifenecker, C. Signarbieux, M. Ribrag, J. Poitou, and J. Matuszek, Nucl. Phys. A189 (1972) 285.

[10] W. John, J. J. Wesolowski, and F. Guy, Phys. Lett. 60 (1969) 340.

[11] J. H. Hamilton, A. V. Ramayya, S. J. Zhu, G. M. Ter-Akopian, Yu. Ts. Oganessian, J. D. Cole, J. O. Rasmussen, and M. A. Stoyer, Prog. Part. Nucl. Phys. 35 (1995) 635.

[12] Y. X. Luo, J. O. Rasmussen, J. H. Hamilton, A. V. Ramayya, J. K. Hwang, C. J. Beyer, S. J. Zhu, J. Kormicki, X. Q. Zhang, E. F. Jones, P. M. Gore, T. N. Ginter, K. E. Gregorich, I-Yang Lee, A. O. Macchiavelli, P. Zielinski, C. M. Folden III, P. Fallon, G. M. Ter-Akopian, Yu. Ts. Oganessian, A. V. Daniel, M. A. Stoyer, J. D. Cole, R. Donangelo, S. C. Wu, and S. J. Asztalos, Phys. Rev. C 66 (2002) 014303.

[13] Y. X. Dardenne, R. Aryaeinejad, S. J. Asztalos, B. R. S. Babu, K. Butler-Moore, S. Y. Chu, J. D. Cole, M. W. Drigert, K. E. Gregorich, J. H. Hamilton, J. Kormicki, I. Y. Lee, R. W. Lougheed, Q. H. Lu, W.-C. Ma, M. F. Mohar, K. J. Moody, S. G. Prussin, A. V. Ramayya, J. O. Rasmussen, M. A. Stoyer, and J. F. Wild, Phys. Rev. C 54 (1996) 206.

[14] W. Urban, J. L. Durell, W. R. Phillips, A. G. Smith, M. A. Jones, I. Ahmad, A. R. Barnett, M. Bentaleb, S. J. Dorning, M. J. Leddy, E. Lubkiewicz, L. R. Morss, T. Rząca-Urban, R. A. Sareen, N. Schultz and B.J. Varley, Z. Phys. A 358 (1997) 145.

[15] G. Simpson, J. Genevey, J.A. Pinston, W. Urban, A. Zlomaniec, R. Orlandi, A. Scherillo, I. Tsekhanovich, A.G. Smith, A. Thallon, B.J. Varley, J. Jolie, and N. Warr, Acta Phys. Polonica B 38 (2007) 1321.

[16] M. Sanchez-Vega, H. Mach, R.B.E. Taylor, B. Fogelberg, A. Lindroth, A.J. Aas, P. Dendooven, A. Honkanen, M. Huhta, G. Lhersonneau, M. Oinonen, J.M. Parmonen, H. Penttilä, J. Äystö, J.R. Persson, and J. Kurpeta, Euro. Phys. J. A 35 (2008) 159.

[17] C. T. Zhang, P. Bhattacharyya, P. J. Daly, R. Broda, Z. W. Grabowski, D. Nisius, I. Ahmad, T. Ishii, M. P. Carpenter, L. R. Morss, W. R. Phillips, J. L. Durell, M. J. Leddy, A. G. Smith, W. Urban, B. J. Varley, N. Schulz, E. Lubkiewicz, M. Bentaleb, and J. Blomqvist, Phys. Rev. Lett. 77 (1996) 3743.

[18] J. K. Hwang, A. V. Ramayya, J. H. Hamilton, D. Fong, C. J. Beyer, K. Li, P. M. Gore, E. F. Jones, Y. X. Luo, J. O. Rasmussen, S. J. Zhu, S. C. Wu, I. Y. Lee, M. A. Stoyer, J. D. Cole, G. M. Ter-Akopian, A. Daniel and R. Donangelo, Eur. Phys. J. A 25 (2005) 463.

[19] Y. X. Luo, S. J. Zhu, J. H. Hamilton, A. V. Ramayya, C. Goodin, K. Li, X. L. Che, J. K. Hwang, I. Y. Lee, Z. Jiang, G. M. Ter-Akopian, A. V. Daniel, M. A. Stoyer, R. Donangelo, S. Frauendorf, V. Dimitrov, J. Y. Zhang, J. D. Cole, N. J. Stone, and J. O. Rasmussen, Intl. J. Mod. Phys. E 18 (2009) 1697.

[20] K. Li, J. H. Hamilton, A. V. Ramayya, S. J. Zhu, Y. X. Luo, J. K. Hwang, C. Goodin, J. O. Rasmussen, G. M. Ter-Akopian, A. V. Daniel, I. Y. Lee, S. C. Wu, R. Donangelo, J. D. Cole, W. C. Ma, and M. A. Stoyer, Phys. Rev. C 78 (2008) 044317.

[21] R. Donangelo, J. O. Rasmussen, M. A. Stoyer and J. H. Hamilton, Int. J. Mod. Phys. E 7 (1998) 669.

[22] D. Fong, J. H. Hamilton, A. V. Ramayya, J. K. Hwang, C. Goodin, K. Li, J. Kormicki, J. O. Rasmussen, Y. X. Luo, S. C. Wu, I. Y. Lee, A. V. Daniel, G. M. Ter-Akopian, G. S. Popeko, A. S. Fomichev, A. M. Rodin, Yu. Ts. Oganessian, M. Jandel, J. Kliman, L. Krupa, J. D. Cole, M. A. Stoyer, R. Donangelo and W. C. Ma, Phys. Atom. Nucl. 69 (2006) 1161.

[23] G. S. Popeko, G. M. Ter-Akopian, J. Hamilton, J. Kormicki, A. V. Daniel, Yu. Ts. Oganessian, A. V. Ramayya, J. K. Hwang, A. Sandulescu, A. Florescu, W. Greiner, J. Kliman, M. Morhac, J. Rasmussen, M. A. Stoyer and J. D. Cole, Bull. Russ. Acad. Sci. 63 (1999) 699.

[24] A. V. Daniel, G. M. Ter-Akopian, J. H. Hamilton, A. V. Ramayya, J. Kormicki, G. S. Popeko, A. S. Fomichev, A. M. Rodin, Yu. Ts. Oganessian, J. D. Cole, J. K. Hwang, Y. X. Luo, D. Fong, P. Gore, M. Jandel, J. Kliman, L. Krupa, J. O. Rasmussen, S. C. Wu, I. Y. Lee, M. A. Stoyer, R. Donangelo, and W. Greiner, Phys. Rev. C 69 (2004) 041305.

[25] M. Heffner and M. A. Stoyer, NA-22 Progress report, March 2006 and M. A. Stoyer, NHI Independent Program Review 5th April 2007 (unpublished).

[26] G. Duchêne, F. A. Beck, P. J. Twin, G. de France, D. Curien, L. Han, C. W. Beausang, M. A. Bentley, P. J. Nolan, and J. Simpson, Nucl. Instrum. Methods 432 (1999) 90.

[27] Z. Elekes, T. Belgya, G. L. Molnár, Á. Z. Kiss, M. Csatlós, J. Gulyás, A. Krasznahorkay, and Z. Máté, Nucl. Instrum. Methods 503 (2003) 580.

[28] R. A. Todd, C. Baktash, M. R. Maier, D. C. Radford, and H. Yaver (unpublished).

[29] C. J. Gross et al., Nucl. Instrum. Methods A 450 (2000) 12.

[30] Evaluated Nuclear Structure Data File (ENSDF), http://ie.lbl.gov/databases/databases.html#ENSDF (Sep 2007).

[31] T. R. England and B.F. Rider, ENDF-349, LA-UR-94-3106, (1994).